Application of Microwaves for Nondestructive and High-Efficiency Detection of Wall Thinning Locations in a Long-Distance Metal Pipe

Linsheng Liu[1,*1], Yang Ju[1,*2], Mingji Chen[1] and Daining Fang[2]

[1]*Department of Mechanical Science and Engineering, Graduate School of Engineering, Nagoya University, Nagoya 464-8603, Japan*
[2]*LTCS, College of Engineering, Peking University, Beijing 100871, P. R. China*

This research aims to find an efficient and nondestructive way of detecting the locations of the pipe wall thinning (PWT) in a long-distance metal pipe at open-end condition. Time domain measurement of microwave signals is adopted in the method since microwaves can propagate a long distance with low attenuation in the pipe and reflection occurs at the PWT section. To carry out the measurement, a vector network analyzer and a self-designed coaxial-line sensor were used to generate microwave signals propagating in the pipe. By analyzing the time domain response of the signals and extracting the time of flight (TOF) that corresponds to the PWT location, the locations are quantitatively evaluated after the group velocity of the signals propagating in the pipe was calibrated. In order to approach a pipe with different PWT degrees and locations, three brass pipes with an inner diameter of 17.0 mm and lengths of 453 mm, 455 mm, and 2000 mm, respectively, were used in the experiment. In addition, five joints, which have the length of 17.0 mm and inner diameters from 17.10 to 18.20 mm were also used. The arithmetical mean error of the evaluation for PWT locations is found to be less than 1.7 mm, i.e. less than 0.068% of the length of the corresponding pipe. It indicates that a quite efficient and precise method to remotely and quantitatively evaluate PWT locations in a long-distance pipe has been established.
[doi:10.2320/matertrans.M2011236]

1. Introduction

Metal pipes are used widely in many industries, including oil and gas transportation, chemical industry and various kinds of power plants. Pipe wall thinning (PWT) is one of the most serious defects in the pipelines during their service in those industries.[1–5] In recent years, accidents caused by PWT have been reported frequently around the world, which have caused severe economical loss and social damages. Therefore, efficient and nondestructive detection of PWT defects as well as their quantitative evaluation, especially for long-distance pipes are mandatory for the effective maintenance and the lifetime prediction of the pipelines in order to avoid severe economical and social damages.

The PWT problem is twofold. One is the PWT degree, which means the depth and length of PWT. This is important information concerning the safety and lifetime of pipes. The other is the PWT location, which is important for the detection and maintenance of in-service pipes, especially long-distance pipes. Recently, many researchers have focused on developing nondestructive testing (NDT) techniques for detecting PWT defects, including infrared thermography,[3] X-ray,[6] electrical potential drop,[7] ultrasonic,[8,9] magnetic flux leakage,[10] eddy current method,[11] elastic-plastic finite element analysis[12] and so on. However, they can only inspect a pipe locally except for the hollow cylindrical guided wave (HCGW) of ultrasonic method.[9] For the HCGW method, the ultrasonic energy will attenuate much faster when there are many girth welds on the surface of the pipe,[13] and the HCGW can only propagate a long distance along an isolated pipe. Moreover, all of these methods are difficult to measure long pipes buried under-

ground, or placed in the walls of some concrete buildings, or under other similar conditions. This is the main shortage for the HCGW method, because the ultrasonic energy will attenuate much faster in the pipe surrounded by various kinds of media such as earth, concrete, etc.[14] In reality, all those methods generally take lots of time and labor to inspect a long-distance pipe, and most of them can only measure the PWT degrees locally, i.e., they can only solve part of the first aspect of the PWT problem.

Since microwave can propagate a long distance with quite little attenuation in a low-loss dielectric medium such as air, gas, and gasoline, it can be used to overcome the shortcomings of the aforementioned methods. To microwave NDT, a metal pipe under test (PUT) can be promisingly taken as a circular waveguide,[4,5,15] and all the energy of microwave signals is confined inside the pipe. Therefore the propagation and attenuation of microwave in the pipe are independent of the surrounding conditions of the pipe.

In our previous studies,[4,5] the PWT degrees of a 2 m long pipe were remotely examined and quantitatively evaluated with a high precision using microwave signals generated by a vector network analyzer (VNA) working at frequency domain. Meanwhile, the time domain response of microwave signals, which can be effectively used for detecting fault location, identifying impedance variations in connectors, transmission lines or waveguides, can be derived from inverse fast Fourier Transform (IFFT) of signals obtained at frequency domain. Because a defect in the pipe affects the impedance of the pipe and causes a reflection peak in time domain signals, the time domain measurement of microwave signals was adopted and then the time of flight (TOF) extracted from the time domain signals was used to detect the locations of defects in a metal pipe.

Some studies have adopted time of flight of microwave signals to detect locations of cracks in a metal pipe,[16,17]

---

however, the evaluation of wall thinning, i.e. a shallow defect with the change of the inner diameter of a pipe, is still not carried out. Especially, there is no literature reporting the inspection of metal pipes by microwaves at the open-end condition which is the most common case in the practice, except the Refs. 4, 5). This paper firstly demonstrates the position measurement of wall thinning in open-end pipes utilizing time domain microwave signals.

Fortunately, studies of Piotrowski,[18] Gimenno and Guglielmi,[19] and Adous *et al.*[20] have shown that when a coaxial line is connected directly to a circular waveguide under the rotational symmetry condition, only TM_{0m} modes are excited in the circular waveguide. In this research, we designed a rotationally symmetric coaxial line sensor, and utilized the TOF of microwave to detect the location of PWT defect. The reason for using TOF to detect PWT location is that a PWT defect acts as discontinuity of the impedance of the waveguide, which causes large reflection at the time domain measurement result.

Using a simple measurement instrument that consists of a VNA and the self-designed coaxial-line sensor, reflected signals in the pipe at frequency domain were measured, and time domain signals were derived through their IFFT. Finally, by calibrating the group velocity and analyzing the time domain signals and extracting information of TOFs corresponding to the PWT locations, we have demonstrated a nondestructive method that can deliver an efficient inspection and quantitative evaluation of PWT locations for a long-distance metal pipe.

It should be noted that this paper mainly aims to establish an efficient and stable method to determine the PWT location in a long-distance pipe regardless of the start point and end point of a PWT defect since lengths of PWT defects are normally no longer than the inner diameter of the pipe. After the location is determined, more detailed information such as the start point and end point, as well as the shape of a PWT defect can be evaluated by a further development of the proposed method or by other local detection methods with further advance in accuracy.

2. Experimental Approach

The experimental instrument is composed of a VNA and a coaxial-line sensor developed by ourselves, as shown in Fig. 1(a). The coaxial-line sensor is made from a standard coaxial-line cable and a connector, and it serves as both the transmitting and receiving port of microwave signals. The length of this coaxial-line sensor is $l_a = 52.0$ mm. In order to inspire strong signals in the pipe that is considered as a circular waveguide, the sensor is designed with inner cable to be $d_0 = 6.5$ mm protrudent as shown in Fig. 1(b).

The pipe specimens tested in the experiment, including three pipes with inner diameter of $d_1 = 17.0$ mm, five joints and two connectors, are made of brass. The lengths of the three pipes numbered as P1, P2, and P3 in the experiment are $l_{11} = 453$ mm, $l_{12} = 455$ mm, and $l_{13} = 2000$ mm, respectively, and the wall thickness of the pipes is $t = 1.0$ mm. The five joints with the same length of $l_2 = 17.0$ mm and different nominal inner diameters are utilized together with the two connectors to construct different wall thinning sections in a
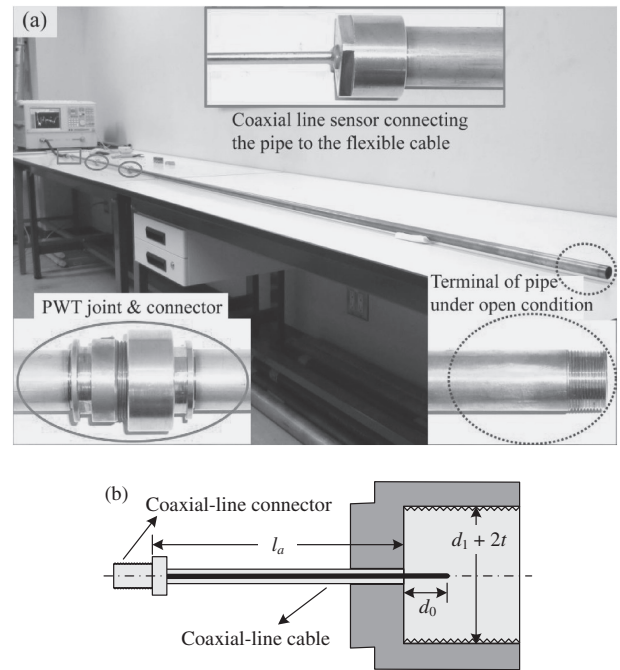

Fig. 1 (a) Overall photograph of experimental instrument (the three insets are the enlarged images of corresponding parts of the pipe, and the correspondence is carried out using markers of real line panes, ellipses, and dashed line ellipses); (b) detailed structure of the self-designed coaxial line sensor.

Table 1   Detailed geometric parameters of the joints.

Joint's number	1	2	3	4	5
Inner diameter, d_2 (mm)	17.10	17.20	17.40	17.80	18.20
PWT degree, %t	5%t	10%t	20%t	40%t	60%t

combined pipe, and they are numbered as joint No. 1 to No. 5 successively and shown in Table 1. Different PWT degrees and locations can be constructed using these pipes, joints, and connectors.

In the experiment, three kinds of pipes with PWT defects of different locations and degrees were constructed by the aforementioned pipes, joints and connectors. The first kind of PUT consists of P1, P3, and a joint located between them, as shown in Fig. 2(a). The difference between the second and the first kind of PUT is the exchange of the locations of pipes P1 and P3. To test the first and second kind of PUT, the five joints listed in Table 1 were connected between P1 and P3 in turn, to construct PWT sections with different PWT degrees. The third kind of PUT is composed of P1, P2, P3, and two joints between them as the photograph shown in Fig. 1(a) and the schematic diagram in Fig. 2(b), which is utilized to approach a pipe with two separate PWT sections. To approach the third kind of PUT, the four joints numbered as No. 1 to 4 in Table 1 are used in the experiment, where one joint (No. 2 to 4, respectively) is used in turn to construct the first PWT section, and the other three joints are used in turn to approach the second PWT section for each joints being used as the first PWT section.

In Fig. 2, l_0 is the total length of the PUT, d_1 is the inner diameter of pipe section without PWT, while t is the wall thickness of the pipe. t_1 and t_2 represent the PWT degrees.
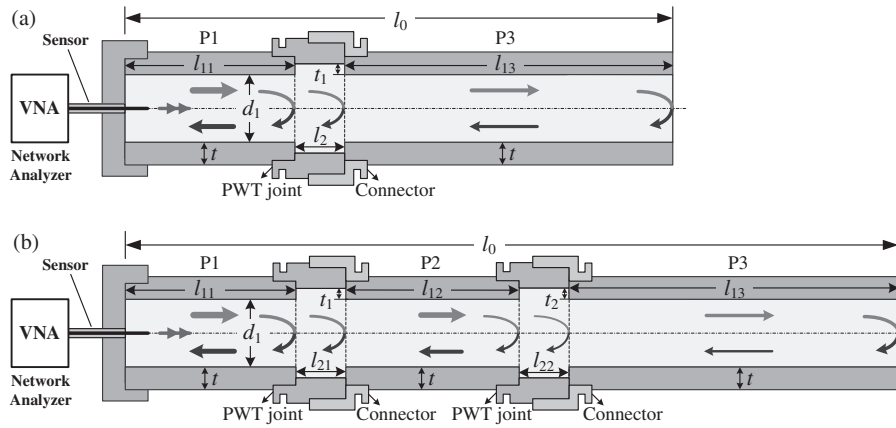
Fig. 2 Schematic diagrams of experimental setup for two groups of combined pipes having (a) single PWT defect near the sensor and (b) two PWT defects.

l_{21} and l_{22} are the corresponding lengths of the two defects, and they are both equal to l_2 in the experiment.

Before measuring the pipe, electrical calibration (E-cal) of one flexible cable of the VNA was carried out to set the zero time reference plane at the end of the flexible cable. During the experiment, microwave signals were generated by the VNA and coupled into the pipe through the coaxial-line sensor. The VNA was set to work at the S11 mode, so that microwave signals reflected from both the PWT sections and the terminal of the PUT were detected by the same port of the sensor. When sweeping the frequency within a proper range, the corresponding amplitudes containing PWT information were measured, and the frequency domain signals were obtained directly, from which the time domain results can be calculated through IFFT. TOF, which is defined as the arrival time of any reflection peak of signals going and returning to the reference zero time interface in this paper, can then be extracted from the time domain analysis of microwave signals.

Moreover, to obtain high precision in the time domain measurement, sweeping points of 1601 are set in the experiment, and the time domain results are designed to be measured in two steps: the first step is to measure the pipe at a very wide range of time domain that is wide enough to contain time domain information from the calibrated zero time interface to the reflection from the terminal of the PUT to get general information of the PWT in the pipe, and the second step is to measure the pipe at a focused range (much narrower range) of time domain where big reflection occurs to obtain more detailed information about the PWT. The two steps are carried out with the same number of sweeping points. Thus, the time precision of the second step is much higher because of the smaller time range is measured. Although it is technically possible to use the maximum 6401 sweeping points, it is found that the result has no obvious difference in the results measured at a focused time range.

3. Theoretical Analysis

3.1 Confirming the range of sweeping frequency

As shown in Fig. 1, the coaxial line sensor is used as both the transmitting and receiving port of microwave signals, and its rotationally symmetric structure when connected to the circular waveguide results to that only TM_{0m} modes are generated,[18-20] among which the dominant mode is TM_{01}.[15] It should be mentioned that, however, the coaxial line sensor used in the experiment is not exactly a coaxial line, but is designed with the inner cable to be $d_0 = 6.5$ mm protruding as shown in Fig. 1(b) so as to inspire strong signals in the pipe. This protrudent structure causes that a comparatively small amount of TM_{nm} modes ($n \neq 0$) other than TM_{0m} modes are also excited in the circular waveguide.

To insure single working mode of microwave signals in the PUT, the sweeping frequency is set to be lower than the cutoff frequency of the first high order mode, i.e. TM_{11} mode. Moreover, because time domain response of the signals is obtained through IFFT of the frequency domain result, the frequency range of signals cannot be too narrow in order to achieve a high resolution in time domain. Therefore, the frequency range between the cutoff frequencies of TM_{01} mode and TM_{11} mode is utilized in the experiment.

The cutoff frequency of TM_{01} and TM_{11} mode are expressed as follows,[15]

$$f_{cTM_{n_01}} = c p_{n_01}/(\pi d), \quad (n_0 = 0, 1) \quad (1)$$

where d is the inner diameter of the pipe, c is the speed of light in free space, and $n_0 = 0$ and 1 correspond to TM_{01} and TM_{11} mode, respectively. p_{n_01} represent the first and the second roots of the first kind Bessel function $J_{n_0}(x)$, i.e. $J_{n_0}(p_{n_01}) = 0$, with $p_{01} = 2.4048$ and $p_{11} = 3.8317$.

3.2 Signal analysis and TOF from the discontinuity of the pipe

The VNA is utilized to generate microwave signals and then measure the frequency domain signals propagating along the pipe. Timed domain response can be mathematically calculated through IFFT of the results of frequency domain response to convert the frequency domain information into the time domain.

For the dominant TM mode, TM_{01} mode, of the circular waveguide, the cutoff wavenumber is $k_c = 2p_{01}/d$. Meanwhile, the wave impedance of a hollow pipe can be derived

from Ref. 15), and the expression shows that the wave impedance is a function of the inner diameter of the pipe. Therefore, change in the diameter of the circular waveguide will cause discontinuity in the wave impedance, and thus the reflection from the location of this discontinuity will occur. This is shown in the schematic diagrams in Fig. 2. The TOFs of the signals reflected from different discontinuities can then be taken as the indications for evaluating the PWT locations.

3.3　Group velocity calibration and PWT location evaluation

The group velocity is a function of the working mode and operating frequencies of microwave in the circular waveguide filled with air and can be expressed as follows,[15]

$$v_g = c \cdot \sqrt{1 - (f_c/f)^2} \propto (1/\lambda_g) \qquad (2)$$

where λ_g is the wavelength in the waveguide and the cutoff frequency is $f_{cTM_{01}} = cp_{01}/(\pi d)$ for the dominant TM_{01}-mode, while f is the operating frequency.

The group velocity of microwave is prerequisite for evaluating PWT locations quantitatively. As mentioned above, to achieve a high resolution in time domain, the operating frequency range of the microwave signals can not be too narrow. Therefore, the group velocity of the wave package which consists of multiple frequencies is difficult to be decided from eq. (2) by a single frequency. In this paper, the group velocity is confirmed using a calibration method.

The calibration of group velocity v_g can be realized by measuring a reference pipe with a known length and exactly the same inner diameter d_1 as the defect-free section of the PUT. When carrying out this calibration, the source signals should be set exactly the same (at the same sweeping frequency range and after the same E-cal) as the ones utilized in the PWT evaluations. The terminal condition of the reference pipe is set to be short circuit by covering the open end of the pipe with a metal cap that can be taken as a perfect conductor. After measuring the TOF corresponding to twice the full length of the reference pipe, the group velocity can be calculated as

$$v_g = 2l_{cal}/T_{end} \qquad (3)$$

where l_{cal} is the length of the reference pipe, and T_{end} is the difference of TOFs corresponding to the signals reflected from the beginning and the end of the pipe. For the pipe at the short circuit condition, a strong reflection will occur at the end of the pipe and cause a large reflection peak in the time domain result, which makes it easy to determine T_{end} with a considerably small error.

Taking the group velocity and the TOF corresponding to the PWT section of the PUT into account, the PWT location can be evaluated by

$$l_{PWT} = v_g \cdot T_{PWT}/2 \qquad (4)$$

where l_{PWT} and T_{PWT} represent the PWT location and TOF corresponding to the PWT, respectively. The presence of factor $1/2$ in eq. (4) is due to the fact that the signals should propagate twice the distance between the sensor and the PWT section after being transmitted and received by the sensor.
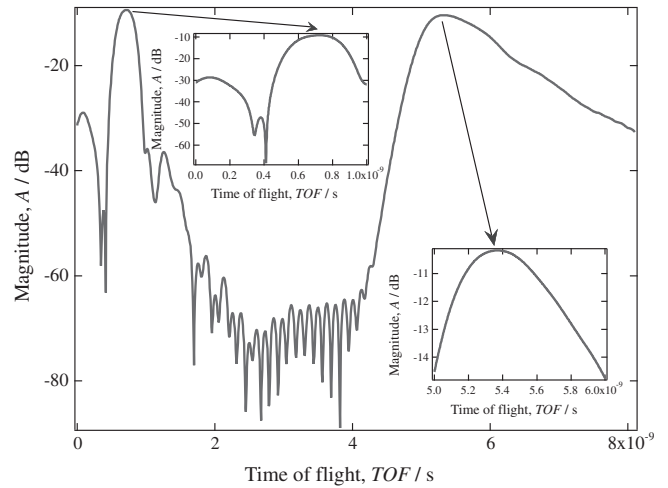

Fig. 3　Time domain experimental results of pipe P1 measured under short circuit condition. To show the results clearer, two figures are inserted: one is the focused figure at time range 0∼1.0 ns for the reflections from the sensor, the other is focus on time range 5.0∼6.0 ns for the reflections from the end of the pipe.

4.　Result Analysis and Discussion

4.1　Analysis of time domain signals and group velocity

For the PUT with inner diameter of 17.0 mm, the cutoff frequencies of TM_{01} and TM_{11} modes are calculated to be 13.499 GHz and 21.509 GHz from eq. (1). To insure the single TM_{01} mode, the sweeping frequency is set to be from 13.0 to 21.0 GHz.

When using pipe P1 to calibrate the group velocity, the experimental results of time domain signals are shown in Fig. 3. It is obtained through IFFT of the frequency domain result. In Fig. 3, quite clear information of the reflections is observed. As mentioned in the experimental approach section, focused measurement of small time range is implemented to improve the precision at time domain, and the obtained results are inserted in Fig. 3. Because the zero time reference plane is set at the end of the flexible cable of the VNA rather than at the beginning of the pipe, the reflection peaks corresponding to all of the connections as well as the reflection from the pipe end are presented together in Fig. 3.

The largest peak at the left side of Fig. 3 is caused by the mismatch between the coaxial-line sensor and the pipe, as the inserted enlarged image of the sensor shown in Fig. 1(a). From the focused result within time range of 0∼1.0 ns shown in Fig. 3, the TOF corresponding to this mismatch is found to be 0.724 ns, which is the TOF at the beginning of the pipe. While the last large peak at the right side of Fig. 3 corresponds to the reflection from the end of the reference pipe P1, and the TOF is measured to be 5.320 ns from the focused result within the time range of 5.0∼6.0 ns.

Therefore, the difference of TOFs corresponding to the signals reflected from the beginning and the end of the pipe is calculated to be $T_{end} = 4.596$ ns. Since the length of pipe P1 is $l_{cal} = 453$ mm, the group velocity is calculated to be $v_g = 1.971 \times 10^8$ m/s from eq. (3).
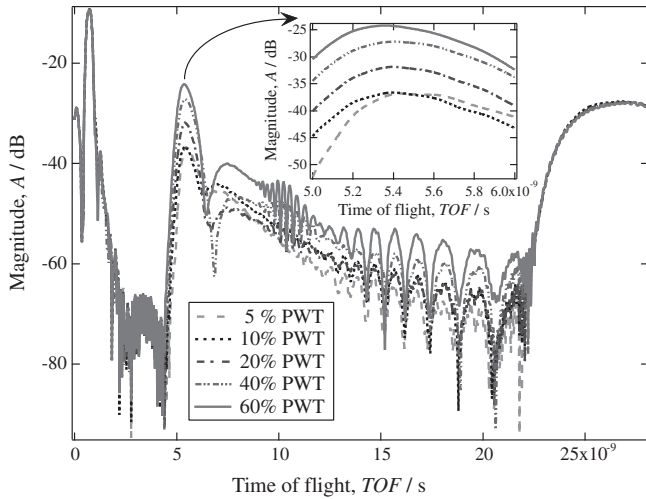
Fig. 4 Experimental results of the combined pipe shown in Fig. 2(a) when connecting with different degrees of PWT joints; the inset figure is the focused part at time range 5.0~6.0 ns around the TOF of reflection from PWT defects.
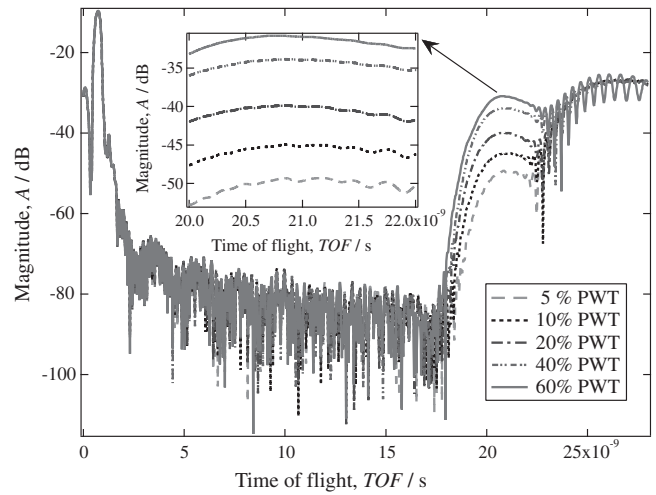

Fig. 5 Experimental results of the pipe composed of pipe P3 and different degrees of PWT joints and then pipe P1; the inset figure is the focused part at time range 20.0~22.0 ns around the TOF of reflection from PWT defects.

4.2 Evaluating the location of a single PWT section

As mentioned above, three kinds of PUT are measured in the experiment. The measurement results of the first kind of PUT in the time domain are shown in Fig. 4. It is found that large reflection peak for each PUT with a different PWT degree occurs around 5.0 ns, which is the TOF from the PWT section. It is shown in both the wide time range result and the focused result within the time range of 5.0~6.0 ns in Fig. 4 that, although the magnitude of the peak corresponding to each PWT section increases with the PWT degree of this section ranging from 50 μm to 600 μm, the TOFs corresponding to these large peaks of reflection are almost the same for all the PWT sections with different PWT degrees. It confirms the ability to detect small PWT defect and the good stability of the proposed method. In addition, a large reflection peak also appears around 25.0 ns, which is caused by the reflection at the open end of the PUT.

However, it should be noted that only one large reflection is observed although there are two discontinuities in the wave impedance, i.e. the discontinuities at the start and end points of a PWT section. This phenomenon is caused by the frequency range being not wide enough, which makes the resolution of time domain measurement being low. When the two reflection peaks caused by the start and end points of the PWT section are not sharp enough, the signals will overlap and, as a result, only the peak of the overlapped signals is observed. Fortunately, the lengths of the industrial PWT defects are generally smaller than the inner diameter of the pipe and of course much smaller than the pipe length. Thus the most important task is the determination of the PWT location in the long-distance pipe rather than distinguishing the start point and end point of the PWT section. After the location is determined, more detailed information such as the start point and end point, and the shape of the PWT defect can be evaluated by an improvement of the proposed method or by other local detection but more accurate techniques. This paper mainly aims to establish an efficient and stable method to determine the PWT location in a long-distance pipe in spite of the detailed structure of the PWT section.
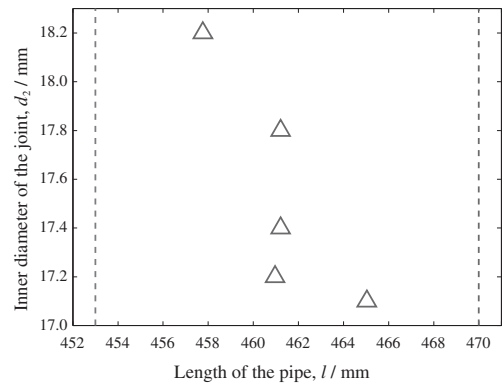

Fig. 6 Evaluated results for the PWT defects located near the sensor shown in Fig. 4.

The measurement results of the second kind of PUT in the time domain are shown in Fig. 5. It is found that large reflection peak for each PUT occurs around 21.0 ns, which is the TOF from the PWT section. Focused result within the time range of 20.0~22.0 ns is shown in the inset of Fig. 5. Similar as the first kind of PUT, the TOFs corresponding to the large reflection peaks are almost the same for the PWT sections with different PWT degrees, which confirms again the good stability of the proposed method.

Taking the calibrated group velocity in pipe P1, i.e. $v_g = 1.971 \times 10^8$ m/s, into account, the PWT locations of the first kind of PUT can be derived from the time domain signals shown in Fig. 4 by eq. (4), and the evaluated results are shown in Fig. 6. In Fig. 6, the values at the abscissa of the two dashed lines correspond to the actual locations of the start point and end point of the PWT section, i.e. 453 mm and 470 mm, respectively.

From Fig. 6, it is found that all the PWT locations evaluated from the TOFs lie between the start and end points of the PWT section. Taking the middle location of the PWT section, i.e. 461.5 mm, as a datum plane, the arithmetical mean error of the evaluation is 1.7 mm, i.e. 0.068% of the length of the PUT, and even the maximum evaluation error is
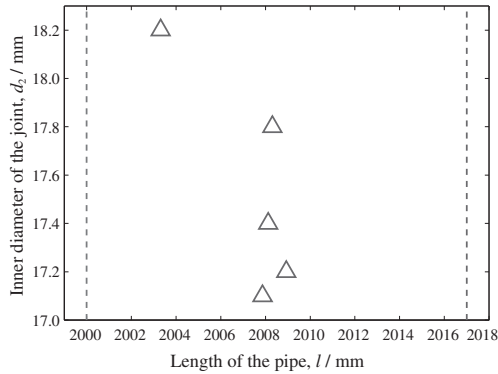
Fig. 7 Evaluated locations for results shown in Fig. 5 of the PWT sections located far away from the sensor.
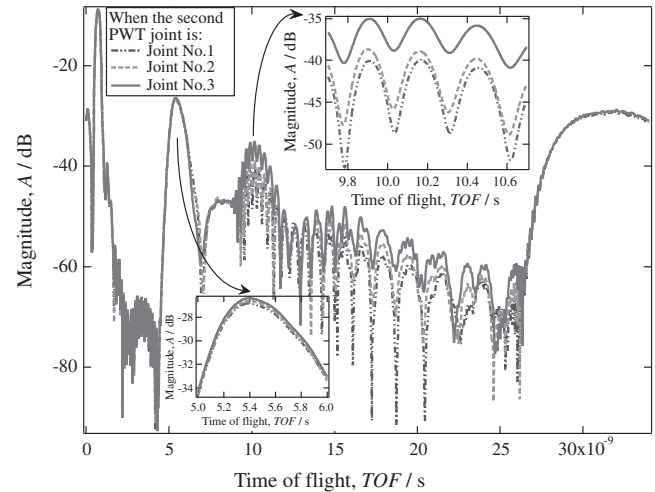

Fig. 8 Experimental results of the pipe composed of pipe P1 and the PWT joint No. 4 and pipe P2 and then PWT joints No. 1~3 and finally pipe P3. The inset figures are the focused part at time range 5.0~6.0 ns around the TOF of reflection from the first PWT defect, and the focused part at time range 9.7~10.7 ns around the TOF of reflection from the second PWT defect.

less than 3.8 mm, i.e. less than 0.16% of the length of the PUT. In addition, it is noted that when the PWT degree is very small such as 50 μm, i.e. 5% of the wall thickness of the pipe, the evaluated location is a little closer to the end point of the PWT section, which means the reflection from the end point is stronger and caused the peak of overlapped signals to lean to the end point; while as the PWT degree is comparatively large such as 0.6 mm, i.e. 60% of the wall thickness, the evaluated location is a little closer to the start point of the PWT section, which is caused by the reflection from the start point becoming stronger.

For the experimental results of the second group of PUT shown in Fig. 5, the group velocity calibration was carried out again using pipe P3 instead of P1 because the pipe P3 is connected to the sensor and located at the beginning of the composite PUT. The group velocity in P3 was obtained as $v'_g = 1.999 \times 10^8$ m/s, and then the PWT locations in the second kind of PUT were evaluated again and shown in Fig. 7.

As shown in Fig. 7, all the PWT locations evaluated are between the start point and end point of the PWT section. Taking the middle location of the PWT section, i.e. 2008.5 mm, as a datum plane, the arithmetical mean error of the evaluation is less than 1.4 mm, i.e. less than 0.055% of the length of the PUT, even for the PWT introduced by the 60% PWT joint, joint No. 5, which has the maximum evaluation error of 5.2 mm, i.e. less than 0.21% of the length of the PUT. It means that all the evaluated locations matches well with the actual values even for the worst one.

As a result of the calibration method, it should be noted that the evaluation results of the proposed method with high precision is sensitive to the calibrated group velocity. In other words, it is very important to calibrate the group velocity by a reference pipe with exactly the same inner diameter with the PUT connected to the sensor. In addition, Fig. 7 is a little different from Fig. 6 that the evaluated location is a little closer to the start point of the PWT section when the PWT degree is as large as 0.6 mm.

4.3 Evaluating the locations of two separate PWT sections

The third kind of PUT is composed of P1, P2, P3 and two joints between them as shown in Fig. 2(b), which is utilized to approach a pipe with two separate PWT sections.

As mentioned in the experimental approach section, the four joints numbered as No. 1 to 4 in Table 1 are used in the experiment, where one joint (No. 2 to 4, respectively) is used in turn to construct the first PWT section, and the other three joints are used in turn to approach the second PWT section. The time domain results of the third kind of PUT with joint No. 4 as the first PWT section is shown in Fig. 8. In Fig. 8, two large peaks caused by reflections from the first and second PWT sections are clearly presented. Similar as the results of PUT with single PWT section, it can also be seen from these figures that the magnitude of the second peak increases with the PWT degree of the second PWT section. On the other hand, the locations of the first and second peaks are almost constant regardless of the different PWT degrees, and this confirms the stability of the proposed method for detecting two separate PWT sections. For conditions that joints No. 2 and 3 were used as the first PWT section, the similar results were obtained, and the only difference is that the magnitudes of the first peaks for them are a little smaller than the results presented in Fig. 8 and, as a result, the reflection signals of the second PWT sections are stronger and the evaluation of them is more feasible. The reason for this phenomenon is that stronger reflection occurs at the first PWT section for the more severe PWT defect, such as joint No. 4, as the first PWT section and, as a result, the stronger reflection caused by the first PWT section more seriously masks the reflection results of the second PWT section.

Considering the group velocity calibrated in pipe P1, i.e. $v_g = 1.971 \times 10^8$ m/s, both the first and second PWT locations can be evaluated by eq. (4) from the time domain results shown in Fig. 8. The evaluated PWT locations corresponding to the results shown in Fig. 8 are shown in Fig. 9, where the dashed lines indicate the start points and end points of the PWT sections. From Fig. 9, it is found that the evaluated locations are almost the same, respectively, for both the first and the second PWT sections, where the errors of the evaluation for both Fig. 9(a) and (b) are less
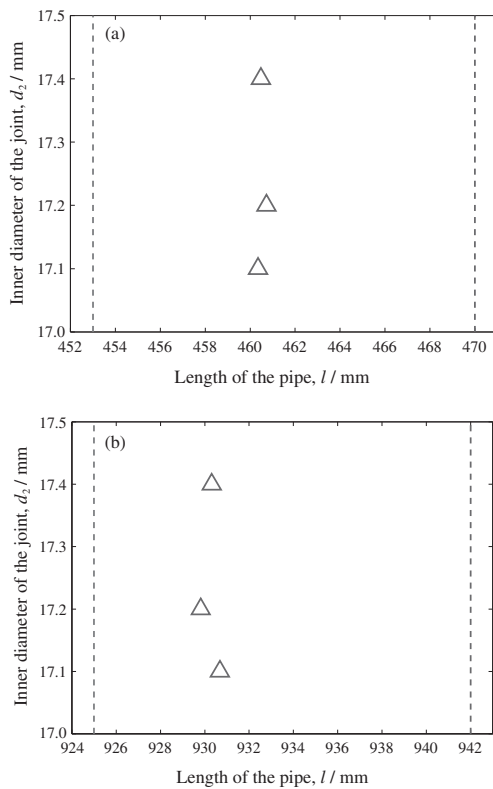
Fig. 9 Evaluated PWT locations for the condition that joint No. 4 as the first PWT defect: (a) Evaluated location for the first PWT; (b) Evaluated location for the second PWT.

than 1.5 mm, i.e. less than 0.06% of the length of the PUT. It means a quite high precision and high stability of the evaluation method has been realized. However, it should be noted that all the evaluated locations of the second PWT sections are not exact the center of the PWT sections but a little closer to the start of these PWT sections.

5. Conclusion

In this research, we have demonstrated an efficient and nondestructive way of detecting the locations of the PWT defects in a long-distance metal pipe at the open-end condition, which is the most common case in the practice.

We achieved this by introducing a self-designed rotationally symmetric coaxial-line sensor used to excite microwave signals of TM_{01} mode in the PUT. Three kinds of pipes under different PWT conditions were used in the experiment and a VNA was used to work at the time domain. The first two kinds of pipes were measured under the condition that each one has only single PWT defect, and the third kind of PUT has two PWT defects. Finally, by analyzing the time domain response of signals and extracting the TOFs corresponding

to the PWT locations, and calibrating the group velocity of microwaves at applied frequencies, the PWT locations were quantitatively evaluated.

The arithmetical mean errors of evaluation for all the three kinds of pipes used in the experiment are found to be less than 1.7 mm, i.e. less than 0.068% of the length of the corresponding pipe. It means that a quite precise and stable evaluation method has been established.

It should be noted that this paper mainly aims to establish an efficient and stable method to determine the PWT location in a long-distance pipe regardless of the start point and end point of a PWT area. This method can not separate the start point and end point of the PWT defect at present because of the resolution of signals, which cause the peaks of reflection to be not very sharp and that only overlapped signals can be detected when the peaks are close to each other. Therefore, after the location is determined, more detailed information such as the start and end points, as well as the shape of a PWT defect is necessary to be evaluated by a further development of the proposed method or by other local detection methods with further advance in accuracy.

REFERENCES

1) R. B. Dooley and V. K. Chexal: Int. J. Pressure Vess. Pip. **77** (2000) 85–90.
2) J. H. Lee and S. J. Lee: NDT & E Int. **42** (2009) 222–227.
3) A. Vageswar, K. Balasubramaniam, C. V. Krishnamurthy, T. Jayakumar and B. Raj: NDT & E Int. **42** (2009) 275–282.
4) L. S. Liu and Y. Ju: NDT & E Int. **44** (2011) 106–110.
5) L. S. Liu: E-Journal Adv. Mainten (EJAM) **2** (2010) 101–109.
6) G. Kajiwara: J. Test Eval. **33** (2005) 295–304.
7) T. Shimakawa, H. Takahashi, H. Doi, K. Watashi and Y. Asada: Nuclear Eng. Des. **139** (1993) 283–292.
8) K. R. Leonard and M. K. Hinders: Ultrasonics. **43** (2005) 574–583.
9) H. Nishino, M. Takemoto and N. Chubachi: Appl. Phys. Lett. **85** (2004) 1077–1079.
10) J. Ding, Y. Kang and X. Wu: NDT & E Int. **39** (2006) 53–56.
11) J. B. Nestleroth and R. J. Davis: NDT & E Int. **40** (2007) 77–84.
12) M. Kamaya, T. Suzuki and T. Meshii: Int. J. Pressure Vess. Pip. **85** (2008) 628–634.
13) Y. Li, L. Sun, Z. Song and Y. Zhang: Ultrasonics. **44** (2006) e1111–e1116.
14) C. Aristégui, M. J. S. Lowe and P. Cawley: Ultrasonics. **39** (2001) 367–375.
15) D. M. Pozar: *Microwave Engineering*, (John Wiley & Sons, N.Y., 1998).
16) K. Abbasi, S. Ito and H. Hashizume: Int. J. Appl. Electromagn. Mech. **28** (2008) 429–439.
17) K. Abbasi, N. H. Motlagh, M. R. Neamatollahi and H. Hashizume: Int. J. Pressure Vess. Pip. **86** (2009) 764–768.
18) J. K. Piotrowski: Proc. 13 Int. Conf. Microw. Radar. Wireless Commun. 2000 (MIKON-2000) 1 (2000) pp. 333–336.
19) B. Gimeno and M. Guglielmi: Int. J. Microw. Millimet. Wave Comput. Aided Eng. **7** (1997) 180–194.
20) M. Adous, P. Queffelec and L. Laguerre: Meas. Sci. Technol. **17** (2006) 2241–2246.